



HAL
open science

Low temperature ionic liquid pretreatment of lignocellulosic biomass to enhance bioethanol yield

Ranim Alayoubi, Nasir Mehmood, Eric Husson, Achraf Kouzayha, Mohamad Tabcheh, Ludovic Chaveriat, Catherine Sarazin, Isabelle Gosselin

► To cite this version:

Ranim Alayoubi, Nasir Mehmood, Eric Husson, Achraf Kouzayha, Mohamad Tabcheh, et al.. Low temperature ionic liquid pretreatment of lignocellulosic biomass to enhance bioethanol yield. *Renewable Energy*, 2020, 145, pp.1808-1816. 10.1016/j.renene.2019.07.091 . hal-02344325

HAL Id: hal-02344325

<https://hal.science/hal-02344325>

Submitted on 21 Dec 2021

HAL is a multi-disciplinary open access archive for the deposit and dissemination of scientific research documents, whether they are published or not. The documents may come from teaching and research institutions in France or abroad, or from public or private research centers.

L'archive ouverte pluridisciplinaire **HAL**, est destinée au dépôt et à la diffusion de documents scientifiques de niveau recherche, publiés ou non, émanant des établissements d'enseignement et de recherche français ou étrangers, des laboratoires publics ou privés.



Distributed under a Creative Commons Attribution - NonCommercial 4.0 International License

1 Nomenclature

A	Surface area, m ²
c_p	Specific heat, J/kg K
$d_{ch.}$	Honeycomb channel diameter, mm
h	Heat transfer coefficient, W/m ² K
K	Thermal conductivity, W/m K
$L_{ch.}$	Axial depth, mm
\dot{m}	Mass flow rate, kg/s
$N_{abs.}$	Number of absorbed photons
N_t	Total number of photons
PPP	Power per photon, W
P_{air}	Rate of heat transfer to air, W
P_{abs}	Absorbed solar power, W
$P_{Sol.}$	Solar power, W
$q_{Sol.}$	Absorbed solar heat flux, W/m ²
$q_{in,k}$	Energy flux incident on the surface k (W/m ²)
$q_{out,k}$	Radiative heat flux leaving surface k (W/m ²)
Q_{conv}	Convective heat losses, W
Q_{rad}	Radiative heat losses, W
S_v	Volumetric heat source, W/m ³
$T_{s,z \rightarrow 0}$	Front wall temperature, K
T	Temperature, K
u	Air velocity, m/s
V_s	Solid volume, m ³

Greek Symbols

α	Absorptivity
β	Incidence angle
ε	Emissivity
Θ_R	Receiver tilt angle
$\eta_{opt.}$	Optical efficiency
$\eta_{Th.}$	Thermal efficiency
μ	Dynamic viscosity, kg/m s
ρ	Density, Kg/m ³
σ	Stefan-Boltzmann constant, W/m ² K ⁴

Subscripts

f	Fluid
in	Inlet
out	Outlet
s	Solid
$amb.$	Ambient
h	heliostat

1. Introduction

Concentrating Solar Power (CSP) is a promising and sustainable technology for electricity generation, chemical fuels production, solar heating and cooling, and water desalination [1–4]. Many types of CSP technologies have been utilized for electricity production such as solar tower power plants (STPPs), parabolic trough, parabolic dish, and linear Fresnel solar collectors [5]. Among the several types of CSP technologies, STPP with open volumetric solar receiver is one of the most promising technologies [6].

STPP is based on the concept of reflecting and concentrating sunlight, using sun-tracking mirrors (heliostats), on the receiver at the top of a central tower. The volumetric solar receiver (VSR) absorbs the solar radiation and converts it to high-temperature heat. Then, a heat transfer fluid (HTF) fluid flows through the receiver and removes the high-temperature heat by forced convection mechanism [7]. This heat is finally used to generate electricity using steam or gas turbine power plants [8]. Air is commonly used as a HTF due to its availability and stability.

In a typical solar tower power plant, VSR is a key element that determines the solar-to-thermal efficiency of the plant. In order to reduce the thermal losses from the VSR to the environment, the outlet temperature of the HTF should be higher than the absorber frontal surface temperature indicating what is referred to in the literature as positive volumetric effect. However, all VSR tested to date show high negative values of volumetric effect [8,9].

Different volumetric solar receivers' designs have been investigated numerically and experimentally. They differ by the structure and the material of the receiver. Both ceramic as well as metallic materials have been tested [10–22]. Different structures include extruded honeycombs with parallel channels [19,20], wire meshes [14,15], ceramic foams [23–27], and printed structures [28]. Silicon carbide (SiC) honeycomb absorber structure has been used in many STPPs such as SolAir3000 power plant [22].

2. Literature survey

Several numerical and experimental studies have been carried out to investigate the optical and thermal performance of VSRs using ceramic honeycombs as an absorber. Figure 1 shows the volumetric solar receiver geometry and the components of a VSR module with honeycomb absorber. Different scales of interaction between optical and thermal phenomena can be envisaged from this figure. Previous numerical studies reported in the literature employed a

1 physical model at the channel scale and focused on analyzing the influence of channel
2 dimensions, such as channel width and wall thickness [29–32] and channel cross-section shape
3 [33] on the performance of the receiver. The important findings of these studies are summarized
4 below.

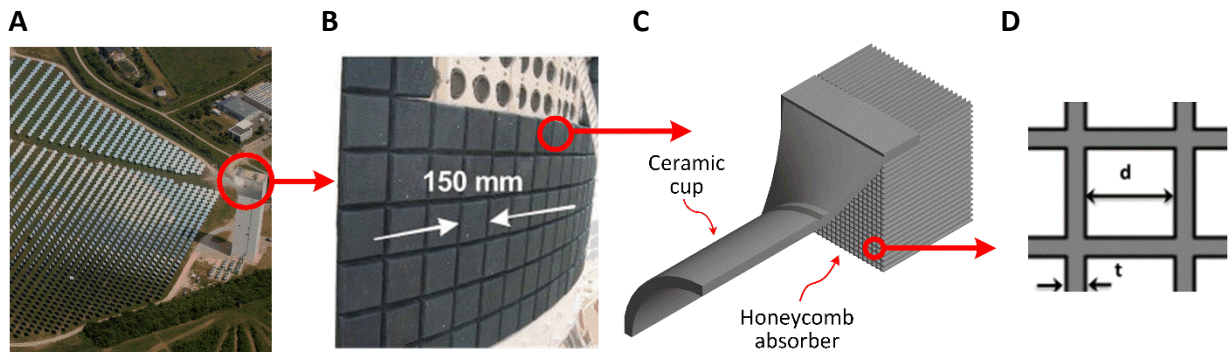


Fig. 1. Central receiver solar plant with honeycomb volumetric absorber: (A) Plant scale [30], (B) Receiver front area [30], (C) Single Module absorber and cup, (D) Channel dimensions

5 Fend et al. [30] carried out numerical and experimental studies to analyze the influence of
6 channel dimensions on the thermal performance of the receiver. Two SiC honeycomb samples
7 with different geometric parameters have been investigated. For sample 1: $d = 2.18$ mm & $t =$
8 0.55 mm and for sample 2: $d = 1.43$ mm & $t = 0.25$ mm. The radiative heat flux distribution on the
9 absorber surface has been estimated using one dimensional Beer Lambert Law (BLL) and has
10 been applied as a heat source in a CFD model using COMSOL software. Their results indicated
11 that the sample with smaller d and t (sample 2) shows better performance in terms of air outlet
12 temperature and thermal efficiency due to the increased specific surface area. However, in both
13 cases, the air outlet temperature was less than the frontal surface temperature of the solid
14 absorber indicating negative values of volumetric effect.

15 Lee et al. [29] used the 3D Monte Carlo ray tracing method (MCRT) and a 1-D CFD model to
16 investigate the influence of channel width (0.5 - 1.5 mm), wall thickness (0.15 – 0.25 mm), and
17 absorptivity ($\alpha = 0.8, 1$) on the performance of the receiver. Their results indicate that increasing
18 the absorptivity leads to a decrease in the reflection losses from the frontal surface of the
19 receiver and enhance the receiver performance. In agreement with Fend et al. [30], they found
20 that honeycomb channels with smaller channel width showed favorable performance in terms
21 of HTF outlet temperature and thermal efficiency. However, Sanchez et al. [31] and Cagnoli et al.
22 [32], using ray tracing code and CFD model, have shown that favorable honeycomb receiver
23 performance has been obtained by increasing the channel width.

1 It should be noted that the previous studies differ in using either simple one-dimensional Beer
2 Lambert law [30,33–35] or 3D Monte Carlo ray tracing [29,32,36] for performing the optical
3 analysis of the receiver and estimating the radiative heat flux distribution on the absorber surface
4 at the scale of single channel dimensions. The later represents the main heat source that may
5 significantly affect the thermal performance of the receiver. Gomez-Garcia et al. [36] show that
6 BLL can be used to describe the radiative heat flux distribution within the honeycomb structure
7 near the entrance of the channel only for depths below two pitches. Moreover, BLL neglects the
8 direction effects of the incoming solar rays as well as rays scattering inside the honeycomb
9 channel. Therefore, using BLL may lead to improper characterization of the radiative flux
10 distribution and overestimation of the HTF outlet temperature. Further analysis to clarify these
11 points and in-depth analysis for the proper choice of the solution domain for consistent
12 numerical modeling of the coupled optical and thermal phenomena inside the receiver represent
13 one of the main objectives of the present article.

14 Previous studies focused on using a material with high absorptivity (SiC) to reduce the
15 reflection losses from the frontal surface of the receiver and increase the optical efficiency [32].
16 Numerical studies carried out by Yilbas and Shuja [33] and Kasaeian et al. [37] indicate that cell
17 configuration with triangular channel cross-section results in higher air outlet temperature and
18 higher thermal efficiency and then followed by square, rectangular, hexagonal, and circular cross-
19 sections. However, negative values of volumetric effect have been observed for all shapes of
20 channel cross-sections evaluated. Gomez-Garcia et al. [36] performed a numerical optical study,
21 using MCRT method, and show that an increase in the penetration depth of concentrated solar
22 radiation can be obtained by using a novel solar receiver composed of a stack of thick square
23 grid.

24 In order to achieve the required positive volumetric effect and high solar-to-thermal-
25 efficiency, radiation propagation within the honeycomb receiver should be maximized [8]. Both
26 the architecture and the high absorptivity of SiC honeycombs limits radiation propagation inside
27 the honeycomb channel. As a result, the maximum penetration depth of the absorbed heat flux
28 is usually less than 3.3 times the channel width [29]. This leads to higher temperature at the
29 frontal surface of the receiver, higher emission losses, lower solar-to-thermal efficiency, and
30 lower air outlet temperature.

31

1 **3. Outline and Contribution of Present Work**

2 The major contributions of the present article and significant differences with previous reported
3 work can be summarized as follows:

- 4 • Consistent numerical modeling of the coupled optical and thermal phenomena inside
5 the volumetric receiver including proper solution domain, boundary conditions, optical
6 modelling, radiation effects, and absorbed solar radiation distribution.
- 7 • Demonstration of the basic concepts to obtain positive values of volumetric effect and
8 high solar-to-thermal efficiency for volumetric receivers. The essential requirement is
9 shown to increase radiation propagation within the honeycomb receiver. However,
10 both the architecture and the high absorptivity of SiC honeycombs have been shown
11 to limit radiation propagation inside the honeycomb channel.
- 12 • An efficient method to maximize the penetration depth within the honeycomb
13 absorber is introduced by judicious control of the absorptivity of the honeycomb
14 channel along its length. Of course, the solar absorptivity of the frontal surface should
15 be as maximum as possible to reduce the reflection losses. However; the absorptivity
16 of the internal walls can be controlled to achieve the required radiation flux
17 distribution and obtain favorable temperature distributions. According to the author's
18 knowledge, this method has not been yet studied in previous research work.
- 19 • A novel honeycomb receiver made of Alumina has been introduced by using judicious
20 surface coating of the absorber material. The coating has been designed with the
21 objective of reducing the reflection losses from the frontal surface and increasing the
22 penetration depth of the absorbed solar heat flux inside the honeycomb receiver
23 channel. The new introduced coated Alumina honeycomb absorbers show a favorable
24 receiver performance in terms of air outlet temperature and solar-to-thermal
25 efficiency compared to conventional SiC honeycomb absorbers.
- 26 • The proposed method can be applied to improve the performance of honeycomb
27 volumetric receivers.

28 The present article is organized as follows: section 4 describes the physical model for the
29 optical and CFD analysis. The heat transfer and Fluid Flow Modeling are illustrated in section 5.
30 In section 6, the results of coupled optical and thermal models are presented and discussed.
31 Conclusions and key findings of the present study are presented in section 8.

4. Physical Models for Optical and CFD Analysis

Actually, the physical model for solar tower power plant consists of sun-tracking mirrors (heliostats) reflecting and concentrating sunlight on the receiver. However, in laboratory testing, solar furnace facilities are used to investigate the thermal and optical performance of VSRs due to high concentration ratios and high temperatures that can be achieved by these systems [38]. As shown in Fig. 2, the solar furnace used in the present study is similar to the facility used in [24] and composed of a reflector, a parabolic concentrator, and a VSR target similar to the one used in SolAir 3000. The total surface area of the reflector and the concentrator are 27 m² and 13.5 m², respectively. The focal distance of the concentrator is 3.8 m. The solar furnace system redirects and focuses the incoming sunlight onto the receiver module surface. The total depth of the absorber (Z) is 50 mm with channels of square cross-section. The honeycomb absorber receives the radiative flux and converts it to high-temperature heat. Then, air flows through the receiver and removes the thermal energy by forced convection.

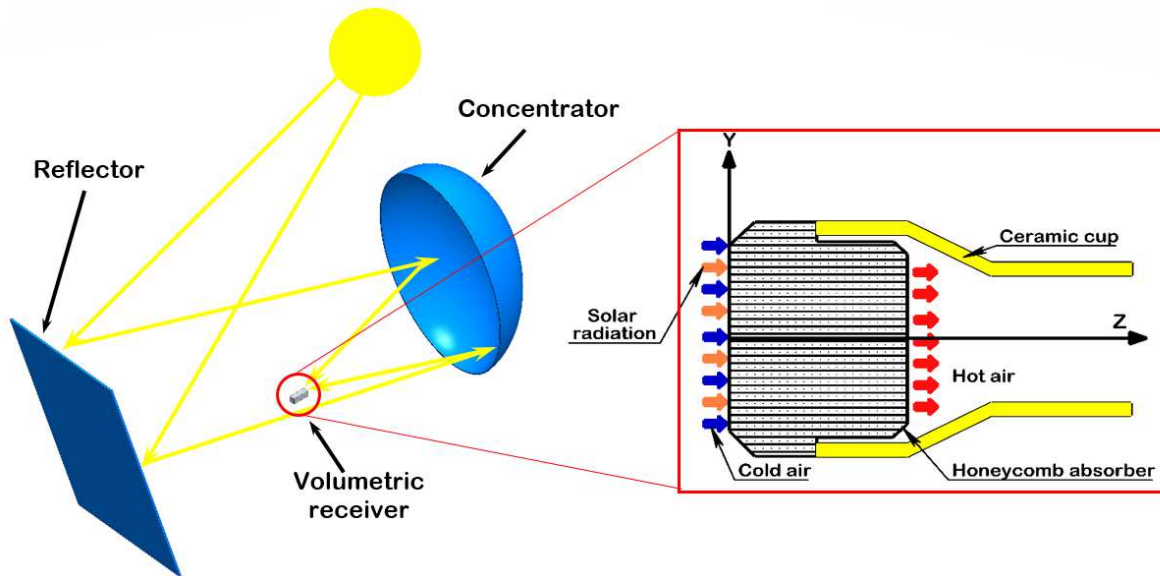


Fig. 2. Schematic diagram of the solar furnace optical model with volumetric solar receiver module.

The solar furnace optical model for the system shown in Fig. 2 has been developed using an experimentally validated object-oriented Monte Carlo based ray tracing software (Tonatiuh[®]) [39–41]. In a typical Tonatiuh ray-tracing simulation, the solar power is discretized into photons. Each photon has the same amount of energy that represents the power per photon (PPP), which is calculated using:

$$PPP = \frac{P_{Sol.}}{N_t} \quad (1)$$

1 Where $P_{Sol.}$ is the solar power and N_t is the total number of photons. The sun shape has been
2 considered as pillbox and the value of direct normal irradiation (DNI) used in the present analysis
3 is 1000 W/m^2 . Since the surface area of the receiver is smaller than the solar image reflected
4 from the concentrator, it can be assumed that the frontal surface of the receiver (A) has a
5 constant flux distribution. The area-averaged absorbed solar heat flux $q_{Sol.}''$ that will be used as a
6 source term for heat transfer analysis has been computed using:

$$7 \quad q_{Sol.}'' = \frac{PPP \times N_{abs.}}{A} \quad (2)$$

8 Where $N_{abs.}$ is the number of absorbed photons. A sensitivity analysis has shown that a
9 minimum number of 10^8 photons is required to reach an independent value of absorbed heat
10 flux at the frontal area of the honeycomb receiver.

11 The ray-tracing algorithm is used to trace and collect the absorption and scattering data of the
12 simulated photons through the system, starting from the light source (the sun) going towards the
13 reflector, the concentrator and finally reaching the receiver. Ray tracing is also used for tracking
14 the paths of the simulated photons through the receiver until they exit it or completely absorbed.
15 This allows to determine the absorbed heat flux at each surface of the honeycomb channels
16 (upper, lower, right, and left surfaces). Complete description of the optical model and analysis of
17 results have been reported by the present authors elsewhere [27].

18 Tonatiuh has been designed to simulate either specular or diffuse surface behavior. The
19 reflection mechanism of a real ceramic material depends on the manufacturing process. It is
20 neither purely specular nor purely diffuse, but it is a mixture of the two. The effects of specular
21 and diffuse reflectivity on the accuracy of the optical model have been addressed before by
22 Cagnoli et al. [32]. The results show that the assumption of specular reflection is accurate enough
23 to reproduce the actual receiver behavior. In the present study, specular directional reflectivity
24 has been implemented in Tonatiuh.

25 The optical analysis showed that the absorptivity of the material plays a dominant role in
26 determining the radiative flux distribution on the honeycomb receiver surfaces. Also, the
27 radiative flux distribution of honeycomb absorbers is highly non-uniform with prominent peaks
28 and surface dependent. The latter finding is very important for consistent coupling of optical and
29 CFD models. This variation of solar heat flux distribution should be properly included in the choice

1 of physical model for CFD analysis. In the previous numerical studies [30,35], only one-quarter of
2 the honeycomb structure cells is used as a solution domain. This choice is valid only when the
3 absorbed heat flux distributions on all honeycomb structure surfaces are identical. Therefore, in
4 this study, an appropriate solution domain has been used as depicted in Fig. 3. The proposed
5 solution domain allows the authors to set the absorbed heat flux of each surface as a standalone
6 one in consistency with the optical analysis. Further details on the governing equations of CFD
7 analysis, boundary conditions implementations and mesh generation are outlined in Section 3.

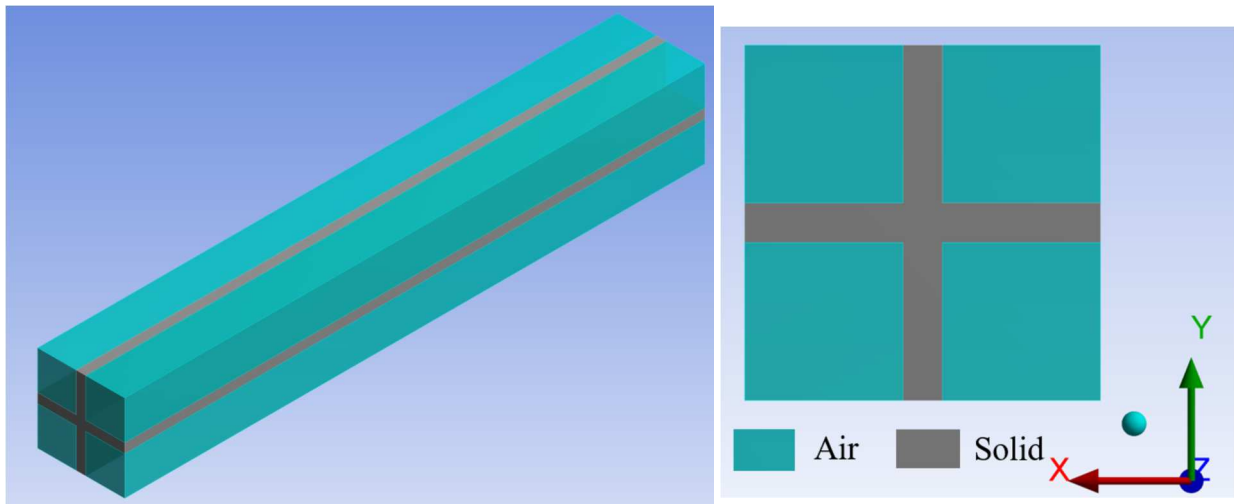


Figure 3. CFD solution domain.

8 5. Heat transfer and Fluid Flow Modeling

9 5.1 Governing Equations

10 The complete model of volumetric solar receiver couples the fluid dynamics and the conjugate
11 heat transfer physics. In the present study, ANSYS[®] software has been used for numerical
12 modeling of the CFD phenomena inside a single channel of the numerical solution domain shown
13 in Fig. 3. The solution domain comprising both fluid and solid domains has been discretized using
14 ANSYS[®] meshing software. The grid consists of tetrahedron elements as shown in Fig. 4. In
15 comparison with hexahedron elements, tetrahedron elements are more efficient, require less
16 computation demand, but are more complex to generate. In addition, five inflation layers placed
17 in the fluid domain at the interface with the solid domain in order to solve the boundary layer
18 where large velocity and temperature gradients usually exist. As a measure of the mesh quality,
19 the Skewness control has been adopted. The Skewness is a measure of the relative distortion of
20 an element compared to its ideal shape and is scaled from zero (Excellent) to one (unacceptable).



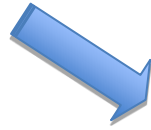
Cellulose



Spruce sawdust



Oak sawdust



Low IL-pretreatment:
[Emim][OAc]
45 °C
40 min



Ethanol yield
increases 2.6 to
3.9 times